Convergence Analysis of Fine Mesh Rebalance Method Coupled with LDEM-SCB(1) for Diffusion Equation

Habib Muhammad, Ser Gi Hong*
Department of Nuclear Engineering, Kyung Hee University: 1732 Deogyeong-daero, Giheung-gu, Yongin, Gyeonggi-do, 446-701, Korea
**Corresponding author: sergihong@khu.ac.kr*

1. Introduction

In this paper, a three-dimensional Fourier analysis of the fine mesh rebalance (FMR) acceleration [1] of the subcell diffusion equations [2] discretized with LDEM-SCB(1) [3] is presented to understand convergence behaviour of the acceleration method. The Fourier analysis is performed by applying the same procedure using the translated quantities on the external boundaries of the basic elements as suggested by J. S. Warsa et al [4]. In addition, the Fourier analysis is newly performed with the reflective boundary conditions for homogeneous test problems.

2. Theory and Formulations

2.1. LDEM-SCB(1) Discretized Diffusion Equation

In our previous work [2], four subcell diffusion equations were derived by consistently discretizing the continuous diffusion equations to the LDEM-SCB(1) method for solving neutron transport equations. The discretized diffusion balance equation over the subcell 1 in the tetrahedral mesh *k* is given by

$$\begin{aligned}
&\left\{22\left(\left|\vec{A}_2^k\right|+\left|\vec{A}_3^k\right|+\left|\vec{A}_4^k\right|\right)+\frac{24D^k}{V^k}\left(\vec{A}_1^k\cdot\vec{A}_1^k\right)+225\sigma_a^k V_{sc1}^k\right\}\phi_1^{k,(\ell+1/2)}\\
&+\left\{7\left(\left|\vec{A}_3^k\right|+\left|\vec{A}_4^k\right|\right)+\frac{24D^k}{V^k}\left(\vec{A}_1^k\cdot\vec{A}_2^k\right)+69\sigma_a^k V_{sc1}^k\right\}\phi_2^{k,(\ell+1/2)}\\
&+\left\{7\left(\left|\vec{A}_2^k\right|+\left|\vec{A}_4^k\right|\right)+\frac{24D^k}{V^k}\left(\vec{A}_1^k\cdot\vec{A}_3^k\right)+69\sigma_a^k V_{sc1}^k\right\}\phi_3^{k,(\ell+1/2)}\\
&+\left\{7\left(\left|\vec{A}_2^k\right|+\left|\vec{A}_3^k\right|\right)+\frac{24D^k}{V^k}\left(\vec{A}_1^k\cdot\vec{A}_4^k\right)+69\sigma_a^k V_{sc1}^k\right\}\phi_4^{k,(\ell+1/2)}\\
&=V_{sc1}^k\left\{225q_1^k+69\left(q_2^k+q_3^k+q_4^k\right)\right\}+\sum_{j=2}^{4}\Theta_j,
\end{aligned}\tag{1}$$

where the term Θ_j is defined by

$$\begin{aligned}
\Theta_j=&\left|\vec{A}_j^k\right|\left\{22\phi_{\alpha'}^{k'(j),(\ell')}+7\left(\phi_{\gamma'}^{k'(j),(\ell')}+\phi_{\delta'}^{k'(j),(\ell')}\right)\right\}\\
&-24D^{k'(j)}/V^{k'(j)}\left\{\sum_{j'=1}^{4}\left(\vec{A}_j^k\cdot\vec{A}_{j'}^{k'(j)}\right)\phi_{j'}^{k'(j),(\ell')}\right\},
\end{aligned}\tag{2}$$

where D is $1/3\sigma_t$, σ_t and σ_a are the macroscopic total and absorption cross-sections, respectively, V_{sc1}^k is the volume of subcell 1, $\vec{A}$ is the face area vector whereas ϕ and $\vec{J}$ represent the scalar flux and the current, respectively. The discretized subcell equations represent a discontinuous discretization of the diffusion equation and we solve them using a GS-like iteration which is represented by the iteration index (ℓ) in Eqs. (1) and (2).

2.2 Fine Mesh Rebalance Method

The rebalance method is one of the earliest acceleration methods used in the neutron transport problems and it has widely been used due to its simple and easy implementation for various transport discretization methods [5-7]. In our previous work, we suggested a linear FMR method [1] to accelerate the GS-like iteration of the discretized diffusion equation over a tetrahedral mesh *k*. The balance equation over the tetrahedral mesh *k* is given by.

$$\begin{aligned}
&T_1^k\phi_1^{k,(\ell+1)}+T_2^k\phi_2^{k,(\ell+1)}+T_3^k\phi_3^{k,(\ell+1)}+T_4^k\phi_4^{k,(\ell+1)}\\
&-\sum_{j=1}^{4}\xi_j^{k,(\ell+1)}=3V^k\left(q_{sc1}^k+q_{sc2}^k+q_{sc3}^k+q_{sc4}^k\right),
\end{aligned}\tag{3}$$

where the terms T_j^k and $\xi_j^{k,(\ell+1)}$ on face *j* are define by

$$T_j^k=3\sigma_a^k V^k+\sum_{\substack{i=1\\ i\neq j}}^{4}\left|\vec{A}_i^k\right|+\frac{\tilde{D}^k}{12}\sum_{i=1}^{4}\left(\vec{A}_i^k\cdot\vec{A}_j^k\right),\tag{4}$$

$$\begin{aligned}
\xi_j^{k,(\ell+1)}=&\left|\vec{A}_j^k\right|\left(\phi_{\alpha'}^{k'(j),(\ell+1)}+\phi_{\beta'}^{k'(j),(\ell+1)}+\phi_{\gamma'}^{k'(j),(\ell+1)}\right)\\
&-\frac{\tilde{D}^{k'(j)}}{12}\sum_{i=1}^{4}\left(\vec{A}_j^k\cdot\vec{A}_i^{k'(j)}\right)\phi_i^{k'(j),(\ell+1)}.
\end{aligned}\tag{5}$$

For the linear FMR method, the additive rebalance factor $\gamma^{k,(\ell+1/2)}$ for the scalar flux is introduced as follows:

$$\phi_j^{k,(\ell+1)}=\phi_j^{k,(\ell+1/2)}+\gamma^{k,(\ell+1/2)}.\tag{6}$$

Substitution of Eq. (6) into Eq. (3) gives following final linear rebalance equation over the mesh *k*:

$$3\left\{\sum_{j=1}^{4}\left(\left|\vec{A}_j^k\right|\right)+4\sigma_a^k V^k\right\}\gamma^{k,(\ell+1/2)}-3\sum_{j=1}^{4}\left(\left|\vec{A}_j^k\right|\gamma^{k'(j),(\ell+1/2)}\right)$$
$$=12\bar{q}^k V^k-\sum_{j=1}^{4}T_j^k\phi_j^{k,(\ell+1/2)}+\sum_{j=1}^{4}\xi_j^{k,(\ell+1/2)}, \tag{7}$$

where $\gamma^{k'(j),(\ell+1/2)}$ is the rebalance factor for the neighbouring mesh $k'(j)$. The rebalance equations compose a system of linear equations whose matrix is symmetric positive definite. We iteratively solved the rebalance equations with a preconditioned conjugate gradient method.

2.3 Fourier Analysis

In this section, we present a three-dimensional Fourier analysis on tetrahedral meshes to theoretically understand the convergence of the FMR method with the translation [4] and the reflective conditions. The basic element is divided into six tetrahedral meshes of equal volume as shown in Fig 1. The Fourier analysis is applied to one basic element and the element is assumed to be repeated with the translation and the reflective conditions.

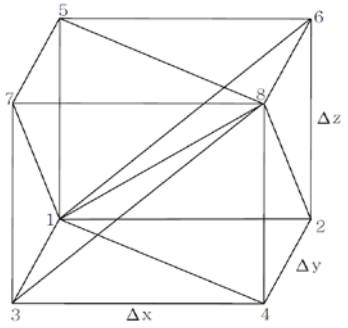

Figure 1: Subcell division for LDEM-SCB(1)[3]

The three-dimensional Fourier ansatz for the diffusion and the FMR equations are defined by

$$\phi_j^{k,(\ell)}=\omega^\ell b_j^k\left(\vec{r}_j^{\,k}\right)e^{i\left(\vec{\Lambda}\cdot\vec{r}_j^{\,k}\right)}, \tag{8}$$

$$\phi_j^{k,(\ell+1/2)}=\omega^\ell a_j^k\left(\vec{r}_j^{\,k}\right)e^{i\left(\vec{\Lambda}\cdot\vec{r}_j^{\,k}\right)}, \tag{9}$$

$$\phi_j^{k,(\ell+1)}=\omega^{\ell+1} b_j^k\left(\vec{r}_j^{\,k}\right)e^{i\left(\vec{\Lambda}\cdot\vec{r}_j^{\,k}\right)}, \tag{10}$$

$$\gamma^{k,(\ell+1/2)}=\omega^\ell d^k\left(\vec{r}_c^{\,k}\right)e^{i\left(\vec{\Lambda}\cdot\vec{r}_c^{\,k}\right)}, \tag{11}$$

where ϕ_j^k is the scalar flux at the local node *j* of the mesh *k*, and γ^k is the additive rebalance factor. In the above equations, $a(\vec{r})$, $b(\vec{r})$, and $d\left(\vec{r}_c^{\,k}\right)$ are the amplitude functions, ω is the eigenvalue, r_j^k is the position, r_c^k is the centric point of the tetrahedral mesh *k*, and $\vec{\Lambda}$ is the vector of Fourier wave numbers. The position vectors r_j^k of the local node point in each mesh are assigned by the global numbers with $i=4(k-1)+j$ to write the quantities at these local nodes in a single vector.

For the translation condition, the incoming terms of Eq. (2) on the tetrahedral meshes that have faces on the external boundary and which exist outside the basic element are represented in terms of the quantities interior to the basic element that are "translated" by the width of the basic element [4]. Similarly, the additive rebalance factors in Eq. (7) from the external face outside the basic element are translated by the terms inside the basic element. Substitution of Eqs. (8) and (9) into the subcell balance equation (i.e., Eq. (1)) gives

$$\mathbf{A}\vec{a}=\mathbf{B}\vec{b}, \tag{12}$$

where the matrices $\mathbf{A}$ and $\mathbf{B}$ are the complex number block matrices each of dimensions 24×24, and the vectors $\vec{a}$ and $\vec{b}$ are of dimensions 24×1.

The submatrices of $\mathbf{A}$ are of dimensions 4×4. The diagonal submatrices are symmetric and originated from the four subcells in each tetrahedral mesh as defined by Eq. (1), whereas, the off-diagonal submatrices are originated from the incoming terms of the upstream meshes as defined by Eq. (2). The off-diagonal submatrices also include the incoming terms from the boundary face translated along the width of the basic element. It is also important to note that if the Jacobi-like-iteration instead of the GS-like one is implemented, then the block matrix $\mathbf{A}$ becomes a block diagonal matrix having no off-diagonal submatrices. The remaining incoming terms and the translated boundary face terms of Eq. (2) compose the submatrices of the block matrix $\mathbf{B}$. The upstream mesh numbering and the mesh sweeping ordering defines the submatrices of $\mathbf{A}$ and $\mathbf{B}$. Eq. (12) can be written as

$$\vec{a}=\mathbf{A}^{-1}\mathbf{B}\vec{b}. \tag{13}$$

Substitution of Eqs. (9) and (11) into the rebalance equation (i.e., Eq. (7)) gives

$$\mathbf{F}\vec{d}=\mathbf{E}\vec{a}, \tag{14}$$

where the vector $\vec{d}$ is of dimensions 6×1. The matrix $\mathbf{F}$ is a complex number matrix of dimensions 6×6 with the elements defined by left hand side of Eq. (7). As the off-diagonal submatrices of $\mathbf{A}$ and $\mathbf{B}$ in Eq. (12) include the incoming terms from the external boundary face translated along the width of the basic element, similarly off-diagonal elements of $\mathbf{F}$ (i.e., the coefficients of the rebalance factors) from the external

boundary face are translated with the ones interior to the basic elements.

The matrix $\mathbf{E}$ is the complex number block matrix with dimensions 6×24 and the submatrices of $\mathbf{E}$ are of dimensions 1×4 originated for the four subcells in each tetrahedral mesh as defined by right hand side of Eq. (7). Eq. (14) can be simplified by substituting Eq. (13) into it as follows:

$$\vec{d} = \mathbf{F}^{-1}\mathbf{E}\mathbf{A}^{-1}\mathbf{B}\vec{b}. \quad (15)$$

Now the substitution of Eqs. (9), (10) and (11) into Eq. (6) gives

$$\omega\mathfrak{R}\vec{b} = \mathfrak{R}\vec{a} + \mathfrak{R}_c\vec{d}, \quad (16)$$

where the matrix $\mathfrak{R}$ is a diagonal matrix and $\mathfrak{R}_c$ is a block diagonal matrix having dimensions of 24×24 and 24×6 respectively.

Substitution of Eqs. (13) and (15) into Eq. (16) gives

$$\omega\vec{b} = \mathbf{M}\vec{b}, \quad (17)$$

where the matrix $\mathbf{M}$ is given by

$$\mathbf{M} = \mathbf{A}^{-1}\mathbf{B} + \mathfrak{R}^{-1}\mathfrak{R}_c\mathbf{F}^{-1}\mathbf{E}\mathbf{A}^{-1}\mathbf{B}. \quad (18)$$

The matrix $\mathbf{M}$ is a function of dimensions $(\Delta x, \Delta y, \Delta z)$ of the basic element, the position of each node point, the Fourier wave numbers, and the material properties. This eigenvalue problem i.e., Eq. (17) is solved for a wide range of the Fourier wave numbers using the power method giving the largest eigenvalue for each combination of λ_x, λ_y and λ_z, and then the largest eigenvalue of them is the spectral radius.

3. Numerical Test and Results

In this section, three-dimensional Fourier analysis is applied to homogeneous test problems to assess the effectiveness of the FMR acceleration to LDEM-SCB(1) discretization method of diffusion equations on tetrahedral meshes. The spectral radii obtained using the Fourier analysis are compared with the numerical estimations of spectral radii which are calculated with

$$\rho \approx \frac{\left\|\vec{\phi}^{(\ell+1)} - \vec{\phi}^{(\ell)}\right\|_2}{\left\|\vec{\phi}^{(\ell)} - \vec{\phi}^{(\ell-1)}\right\|_2}. \quad (19)$$

The first test problem is a homogeneous basic element of variable dimensions to consider the different minimum aspect ratios and the translation boundary condition. The minimum aspect ratio is defined as the ratio of three times the radius of the inscribed circle to the radius of circumscribed circle1 [4]. Table I shows various minimum aspect ratios of the basic elements of different dimensions. In this test problem, the total cross-section is 1.0 cm^{-1} and the scattering ratio varies from 0.9 to 0.9999. The spectral radii are plotted as decreasing function of minimum aspect ratio as shown in Fig. 2. It is observed from Fig. 2 that the FMR acceleration significantly improves the convergence of the GS-like iteration of LDEM-SCB(1) for various aspect ratios even if the spectral radii increase with the decreasing minimum aspect ratio.

Table I: Minimum Aspect Ratio in terms of Dimensions [4]

#	α_{min}	h_x (cm)	h_y (cm)	h_z (cm)
1	0.632	1.0	1.0	1.0
2	0.562	2.0	2.0	3.0
3	0.487	1.0	1.0	2.0
4	0.421	2.0	2.0	5.0
5	0.370	2.0	1.0	3.0
6	0.327	3.0	1.0	3.0
7	0.256	2.0	1.0	5.0
8	0.170	2.0	1.0	8.0
9	0.116	8.0	1.0	10.0

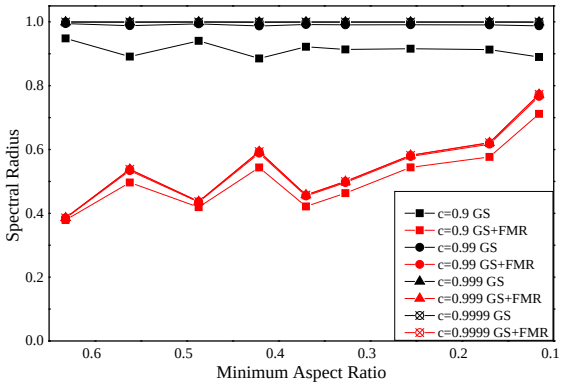

Figure 2: Comparison of Analytical Spectral Radii of GS-like Iteration and FMR

The second test problem is the same as that of the first test problem except the boundary conditions are reflective instead of the translated ones. That's to say, the quantities on the external faces outside the basic element are not translated to the interiors of the basic element, but the reflective conditions are applied on the external boundaries. The spectral radii obtained with the Fourier analysis and reflective condition are compared in Fig. 3 for various scattering ratios.

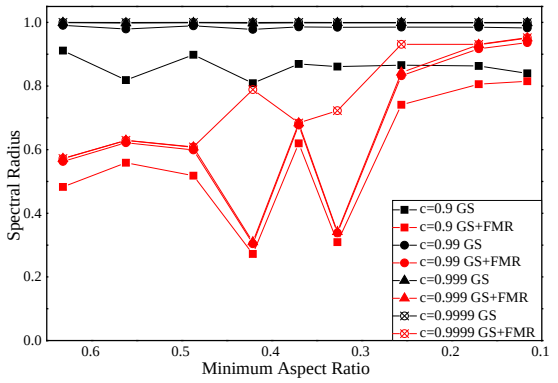

Figure 3: Comparison of Analytical Spectral Radii of GS-like Iteration and FMR Acceleration for Various Minimum Aspect Ratios (Reflective B.C.)

Fig. 3 shows that FMR still accelerates the convergence of the GS-like iteration while the

convergence becomes considerably slower as the minimum aspect ratio decreases. The spectral radii are more sensitive on the minimum aspect ratio than those with translation boundary condition. However, it is noted that the spectral radii with the reflective boundary condition at 0.421 and 0.327 minimum aspect ratios are significantly smaller than those with translation boundary condition.

Next, for first problem, we compare the analytical spectral radii obtained with the Fourier analysis and the numerically estimated ones with Eq. (19) to show the justification of the Fourier analysis with the translation boundary condition. Figs. 4 and 5 show that the analytically and numerically estimated spectral radii of the GS-like iteration and its FMR acceleration for all the minimum aspect ratios nearly agree with each other for all values of the scattering ratios ranging from 0.9 to 0.9999.

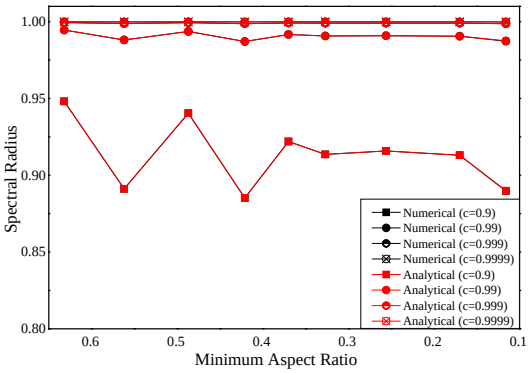

Figure 4: Comparison of the Analytically and Numerically Estimated Spectral Radii (GS-like Iteration with Translation B.C.)

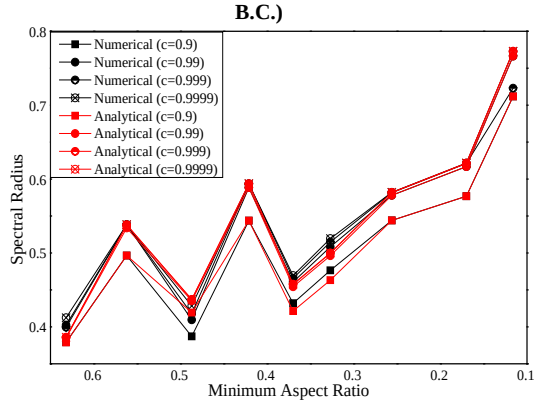

Figure 5: Comparison of the Analytically and Numerically Estimated Spectral Radii (FMR Acceleration of GS-like Iteration with Translation B.C.)

4. Summary and Conclusion

In this work, a three-dimensional Fourier analysis on tetrahedral meshes was successfully performed for homogeneous test problems to theoretically understand the convergence of the GS-like iteration and its FMR acceleration method of the LDEM-SCB(1) method for neutron diffusion equation. The Fourier analysis was performed with translated boundary conditions and also newly with the reflective boundary conditions to show the effect of the boundary condition on the convergence. The results of the Fourier analysis for a homogeneous test problem having different aspect ratios showed that FMR with translated boundary condition leads to overall faster convergence except for few minimum aspect ratios and less sensitive convergence on the minimum aspect ratios than the one with reflective condition. From this problem, it was also shown that FMR with translated condition effectively accelerates the GS-like iteration for all the scattering ratios and for all the minimum aspect ratios and FMR with reflective condition is still effective for all the scattering ratios except for very small minimum aspect ratio. The comparison of numerically and analytically estimated spectral radii for this problem justified the three-dimensional Fourier analysis for the GS-like iteration and its FMR acceleration.

5. References

[1]. H. Muhammad and S. G. Hong, “Effective Use of the Linear Fine Mesh Rebalance for the DSA of S_N Transport Equation with Tetrahedral Meshes,” Transactions of the American Nuclear Society, Philadelphia, Pennsylvania, Vol. 118, June 17-21, (2018).
[2]. H. Muhammad, S. G. Hong, “Diffusion Synthetic Acceleration (DSA) for the Linear Discontinuous Expansion Method with Subcell Balance (LDEM-SCB),” Transactions of Korean Nuclear Society, Jeju, Korea, May 16-18, (2017).
[3]. S. G. Hong, “Two Subcell Balance Methods for Solving the Multigroup Discrete Ordinates Transport Equation with Tetrahedral Meshes,” Nuclear Science and Engineering, 173, 101-117 (2013).
[4]. J. S. Warsa, T. A. Wareing, J. E. Morel, “Fully Consistent Diffusion Synthetic Acceleration of Linear Discontinuous S_N Transport Discretizations on Unstructured Tetrahedral Meshes,” Nuclear Science and Engineering, 141, pp. 236-251 (July 2002).
[5]. M. L Adams and E. W. Larsen, “Fast Iterative Methods for Discrete Ordinates Particle Transport Calculations,” Progress in Nuclear Energy, 40, pp.3-159, (2002). A. Yamamoto, “Generalized Coarse Mesh Rebalance Method for Acceleration of Neutron Transport Calculations,” Nuclear Science and Engineering, 151, pp. 274-282, (2005).
[6]. S. G. Hong, K. S. Kim and J. S. Song, “Fourier Convergence Analysis of the Rebalance Methods for Discrete Ordinates Transport Equations in Eigenvalue Problems” Nuclear Science and Engineering, 164, pp. 33-52, (2010).
[7]. S. G. Hong and N. Z. Cho, “A Rebalance Approach to Nonlinear Iteration for Solving the Neutron Transport Equations,” Annals of Nuclear Energy, 24, pp. 144-160, (1997).